

1 **Application of EGCG modified EDC/NHS cross-linked extracellular**
2 **matrix to promote macrophage adhesion**

3 Chenyu Chu^{a,b,#}, Shengan Rung^{a,b,#}, Renli Yang^{a,b}, Yi Man^{a,b*}, Yili Qu^{a,b*}

4 ^a *State Key Laboratory of Oral Diseases, West China Hospital of Stomatology, Sichuan University,*
5 *Chengdu, Sichuan 610041, China*

6 ^b *Department of Oral Implantology, West China Hospital of Stomatology, Sichuan University,*
7 *Chengdu, Sichuan 610041, China*

8 [#]*theses author contributed equally to this work*

9 **Corresponding author:**

10 **Yi Man, DDS, Ph.D**

11 Professor and Chair

12 Department of Oral Implantology

13 State Key Laboratory of Oral Diseases, West China Hospital of Stomatology, Sichuan University,

14 14#, 3rd section, Renmin South Road

15 Chengdu 610041, China

16 Tel: 0086-28-85503571

17 Fax: 0086-28-85483678

18 Email: manyi780203@126.com

19 **Yili Qu, DDS, Ph.D**

20 Associate Professor

21 State Key Laboratory of Oral Diseases, West China Hospital of Stomatology, Sichuan University,

22 14#, 3rd section, Renmin South Road

23 Chengdu 610041, China

24 Tel: 0086-28-85503571

25 E-mail: qqyili@126.com

26

27 **Abstract:** Though chemically cross-linked by EDC/NHS endows collagen membrane
28 with promising mechanical properties, it is not conducive to modulation of foreign
29 body reaction (FBR) after implantation or guidance of osteogenesis. In our previous
30 research, we have found that macrophages have a strong regulatory effect on tissue
31 and bone regeneration during FBR, and EGCG modified membranes could adjust the
32 recruitment and phenotypes of macrophages. Accordingly, we develop the
33 EGCG-EDC/NHS membranes, prepared with physically immersion, while the surface
34 morphology of the membrane was observed by SEM, the biological activity of
35 collagen was determined by FTIR, the activity and adhesion of cell culture *in vitro*,
36 angiogenesis and monocyte/macrophage recruitment after subcutaneous implantation,
37 etc. are characterized. It could be concluded that EGCG-EDC/NHS collagen
38 membrane is hopeful to be used in implant dentistry for it not only retains the
39 advantages of the collagen membrane itself, but also improves cell viability, adhesion
40 and vascularization tendency. However, the mechanism that lies in the regenerative
41 advantages of such membrane needs further exploration, but it is certain that the
42 differences in surface morphology can have a significant impact on the reaction
43 between the host and the implant, not to mention macrophage in bone regeneration.

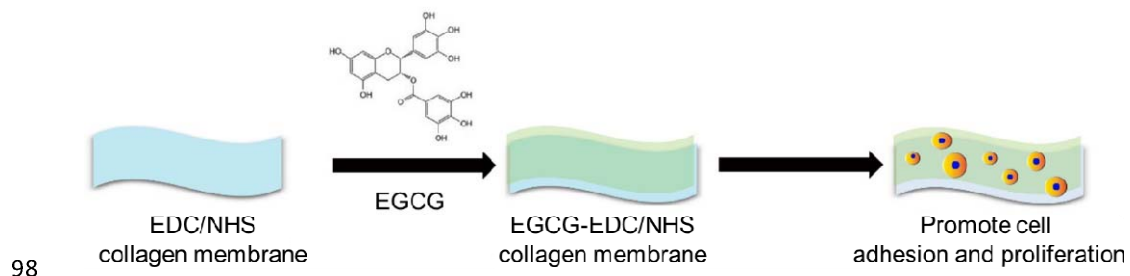
44 **Keywords:** collagen membrane; EGCG; adhesion; macrophage; implant dentistry
45

46 **1. Introduction**

47 Guided bone regeneration (GBR) technology takes advantage of barrier membrane to
48 compartmentalize soft and hard tissue. It protects the hard tissue from an invasion of
49 the relatively fast-growing soft tissue, thus creates sufficient space and provides
50 stability for osteogenic cell migration in the meanwhile (Melcher, 1976). Currently,
51 collagen, the main organic component of extracellular matrix (ECM) and bone, is the
52 most common resorbable source for membrane fabrication. A meta-analysis revealed
53 that the survival rate of implant with the application of collagen membrane were close
54 to 100% both in simultaneous and subsequent implant placement (Wessing, Lettner, &
55 Zechner, 2018). However, its high biocompatibility also becomes its fatal flaw, which
56 limits the mechanical properties of the collagen membrane. Without the addition of
57 crosslinking agents, the integrity of the membrane may not be able to maintain
58 throughout the entire process of bone regeneration to provide sufficient support
59 (Meyer, 2019). Although the exposure of membrane is slightly related to the addition
60 of crosslinker, it is not statistically significant (30%) (Wessing et al., 2018). This
61 observed degradation time is markedly longer than that of collagen membrane, which
62 is reported to be completely resorbed 1 to 2 weeks after exposure [18, 34]. The
63 prolonged degradation time of matrix barrier seems to provide prolonged protecting
64 of the underlying graft supporting the bone regeneration process. During this healing

65 process, all exposures did resolve within 6-7 weeks and no membrane had to be
66 extracted. The ridge width gain in both groups was sufficient to allow for the
67 successful placement of dental implants in all 14 subjects without any complication
68 (Eskan, Girouard, Morton, & Greenwell, 2017). Therefore, to enhance mechanical
69 properties with low cytotoxicity and low antigenicity,
70 1-ethyl-3-(3-dimethylaminopropylcarbodiimide hydrochloride (EDC) in the presence
71 of N-hydroxy-succinimide (NHS) collagen membrane was selected as our target
72 (Akhshabi, Biazar, Singh, Keshel, & Geetha, 2018; Bax et al., 2017). Apart from the
73 degradation rate of membranes, immune environment of the implant site is another
74 factor that determines the success or failure of the surgery (El-Jawhari, Jones, &
75 Giannoudis, 2016). Especially in periodontitis, a chronic and degenerative
76 inflammatory disease which affects approximately 10% of the world's population, the
77 inflammatory environment makes it harder to conduct tissue engineering with
78 biomaterials, thus elevates the importance of immune modulation to rebuild balance
79 (Kurashima & Kiyono, 2017). Epigallocatechin-3-gallate (EGCG) as one of the main
80 polyphenols in tea could serve as a crosslinker for scaffolds (Honda et al., 2018),
81 showing bioactive effects in various aspects, especially in dental restoration (Liao et
82 al., 2020). Compared with pure collagen membrane, its anti-inflammatory (Lagha &
83 Grenier, 2019; Wu, Choi, Kang, Kim, & Shin, 2017), anti-fibrosis (Wang, Yang, Yuan,

84 Yang, & Zhao, 2018), pro-osteogenic (Lin et al., 2018), macrophage phenotypes
85 regulatory (Chu et al., 2019) effects are all prompt to rescue the pro-long
86 inflammation and help the establishment of ideal microenvironment to provide
87 promising signal in regeneration (Chu et al., 2020). Considering its promising traits,
88 EGCG was cross-linked to attach the commercial EDC/NHS collagen, and the
89 modification of EGCG was adjusted at 0.064% w/v, where it is reported to possess
90 appropriate mechanical properties, anti-inflammatory effects, and cell viability
91 promotion in previous report (Chu et al., 2016). To ensure that the developed EGCG
92 modified EDC/NHS collagen membrane meets the need of GBR, its physical,
93 chemical and biological properties was characterized by means of investigation on
94 surface morphology, FTIR spectra, DSC statistics, *in vitro* cell viability and integrin
95 expression, and *in vivo* vascularization and monocyte/ macrophage recruitment. The
96 aim of this study is to fabricate 0.064% EGCG EDC/NHS collagen membranes (**Fig.**
97 **1**) with the improvement of cell viability and adhesion, as well as revascularization.



99 **Fig. 1.** Schematic graph of loading 0.064% EGCG to EDC/NHS collagen membrane

100 **2. Materials and Methods**

101 **2.1 Materials**

102 Commercially available EDC/NHS collagen membranes (Dentium) in size of
103 10mm×20mm were purchased. EGCG was purchased from Jiang Xi Lv Kang Natural
104 Products (Jiang Xi, China). All solvents and chemicals employed in the process were
105 analytical grade and were used without further purification. The EGCG modified
106 EDC/NHS collagen membrane was fabricated as follow: each EDC/NHS collagen
107 membrane was immersed in 0.064% (w/v) EGCG solution at room temperature for 1
108 hr. After that, the EGCG-EDC/NHS collagen membranes were rinsed three times in
109 deionized water and freeze dried overnight. The pure EDC/NHS collagen membranes
110 were also processed under the same protocol except for immersion.

111 **2.2 Surface morphology**

112 The morphologies of EDC/NHS collagen membranes and EGCG modified collagen
113 membranes were characterized by Scanning electron microscope (SEM, S-800,
114 HITACHI, Tokyo, Japan) with an accelerating voltage of 25 kV. The discs were
115 coated with an ultrathin layer (300 Å) of Au/Pt in an ion sputter (E1010, HITACHI,
116 Tokyo, Japan) to achieve enough electrical conductivity.

117 **2.3 Mechanical and chemical properties**

118 a. Mechanical properties measurement

119 To investigate the ultimate stress (US), ultimate elongation (UE) and Young's
120 modulus (YM) of the membranes, each sample (10mm×20mm) was attached to an
121 electronic universal testing machine (SHIMADZU, AG-IC 50 KN, Japan). Five
122 samples were measured for each kind of membranes. Each sample was strained at a
123 rate of 15mm/min at room temperature. When operating differential scanning
124 calorimeter (DSC) measurement, samples in size of 10mm×20mm (~6.71 mg) were
125 encapsulated in aluminum pan, then heated from 25 to 500 °C at a rate of 10 °C/min
126 under nitrogen atmosphere. Thermo-grams were obtained by the Netzsch Proteus
127 analysis software, and thermal denaturation was recorded as the typical peak.

128 b. Chemical properties measurement

129 A Fourier transform infrared spectroscopy (FTIR) spectrophotometer (Spectrum One,
130 PerkinElmer, Inc., Waltham) was employed to measure the FTIR spectra of the
131 samples, the spectra of which were obtained at room temperature at the average of 32
132 scans in the range of 400 – 4000 cm⁻¹.

133 **2.4 Cell viability**

134 The cell viability was examined using the mouse macrophage cell line Raw 264.7
135 obtained from the American Type Culture Collection (Rockville, MD, USA). Staining
136 of Cell Counting Kit-8 (CCK-8, Dojindo Laboratories, Kumamoto, Japan) and
137 Calcein AM/Hoechst were both conducted, but for different time periods. For CCK-8,

138 membranes were processed into 10mm×10mm in the clean bench, then placed in
139 48-well plates and seeded with Raw 264.7 cell at a density of 10^4 /well. 10% CCK-8
140 solution would be added to each well. Cells were then co-cultured for 10, 20, 40, 60,
141 120, 240, 360 min and 1 day, respectively, with RPMI (Gibco, Thermo, USA)
142 supplemented with 10% FBS (Gibco, Thermo, USA). Then plates would be incubated
143 at 37 °C for another 3.5 hr. After incubation, the OD value at 450 nm was measured to
144 determine the cell viability through a micro-plate reader (Multiskan, Thermo, USA).
145 As for staining of Calcein AM/Hoechst, cells were cultured for 5 days on the dishes
146 then incubated with 1μM Calcein AM (diluted from a 1mM stock solution of CAM in
147 dimethyl sulfoxide, Dojindo Laboratories, Kumamoto, Japan) and 100 μL RPMI for
148 30 mins in the incubator. The dishes were then washed three times by 1×PBS and
149 stained with 100μL Hoechst 33258 working fluid (diluted from a 1mL stock solution
150 in distilled water, KeyGen, China) for 10 mins in the incubator. At last, washed the
151 dish for three times by 1×PBS and analyzed with an Inverted Ti-E microscope
152 (Nikon).

153 **2.5 Cell adhesion**

154 SEM images were taken to preliminary estimate cell adhesion after culturing on
155 EDC/NHS-Col and 0.064% EGCG-EDC/NHS-Col for 10, 20, 40 and 480 min, with
156 processed as mentioned in 2.2. The expressions of integrin beta 1, 2, 3 in Raw 264.7

157 cells after culturing on blank wells, EDC/NHS-Col and 0.064%
158 EGCG-EDC/NHS-Col for 10 mins were further evaluated by RNA isolation, cDNA
159 synthesis, and RT-qPCR. Cells cultured on different surfaces were collected after
160 incubating with 0.05% trypsin-EDTA (Gibco, Thermo, USA) for 5 mins and
161 homogenized in 1-ml Trizol Reagent (Tianjian, Beijing, China). Total RNA was
162 reverse-transcribed using mRNA Selective PCR kit (TaKaRa Bio-Clontech). Mouse
163 integrin beta 1, 2 and 3 cDNA were amplified by real-time PCR using the SYBR
164 Green PCR kit (Thermo Scientific, Braunschweig, Germany). The primer sequences
165 used for the real-time PCR were listed in **Table 1**.

166 **2.6 Surgical Procedures**

167 The protocol of the present experiment was approved by Institution Review Board of
168 West China Hospital of Stomatology (No.WCHSIRB-D-2017-097). Male C57BL/6,
169 6~7 weeks of age, were adaptively fed for 3 days after purchasing. After
170 anaesthetization by chloral hydrate, the surgical area on the back was shaved and
171 aseptically prepared. Three parallel sagittal incisions were made in the dorsal skin and
172 subcutaneous pockets were prepared for membrane implantation. The two kinds of
173 membranes were prepared beforehand into 3mm×3mm size in the clean bench.
174 EDC/NHS collagen membranes and EGCG-EDC/NHS collagen membranes were
175 implanted into the pockets respectively. The control group underwent a sham

176 procedure. Afterwards, all the incisions were sutured. These mice were kept in a
177 professional experimental animal room and fed with a standard laboratory diet. After
178 recovering for 0 (12hr), 1, and 3 days, they were sacrificed by cervical dislocation.
179 The membranes and the skins covering the materials were harvested together (equal
180 areas around the suture were harvested in the control groups) and immediately fixed
181 with 4% paraformaldehyde (Solarbio, Beijing, China) for at least 24hr.

182 **2.7 H & E staining**

183 The fixed samples were sliced into 3- μ m thick sections after embedding in paraffin
184 for the following H & E staining and immunofluorescence assay. For H & E staining,
185 the sections were incubated at 65 $^{\circ}$ for 4hr for deparaffinization and processed as
186 follow:

- 187 a. Dhydration with ethanol;
- 188 b. Stain with hematoxylin for 5 mins and differentiate in 1% hydrochloric acid
189 alcohol for 2 s ;
- 190 c. Incubate in 0.2% ammonia water for 2 mins and stain with eosin for 1 min;
- 191 d. Gradual dehydration through 95% ethanol, then clear and mount the sections with
192 neutral resin. The sections were observed with light microscopy (Olympus, Tokyo,
193 Japan) and scanned with Digital Slide Scanning System (PRECICE, Beijing,
194 China).

195 **2.8 Promotion of revascularization**

196 3 days after implantation, tissue was harvested and prepared as sections. Then,
197 sections would be fixed with 2% paraformaldehyde PBS for 24 hours (pH=7.4) and
198 later washed by PBS for 3 times, which followed by soaking in 1% bovine serum
199 albumin (BSA) PBS that contained 1% Triton X-100 for 1 hour. Eventually, incubated
200 the sections in 1% Tween 20 for 10 mins, and washed twice in PBS for 5 mins. The
201 sections were then stained with nucleus marker Hoechst, endothelial cell marker
202 CD31 and adventitial fibroblast marker α -SMA to visualized specific components in
203 the fluorescent images.

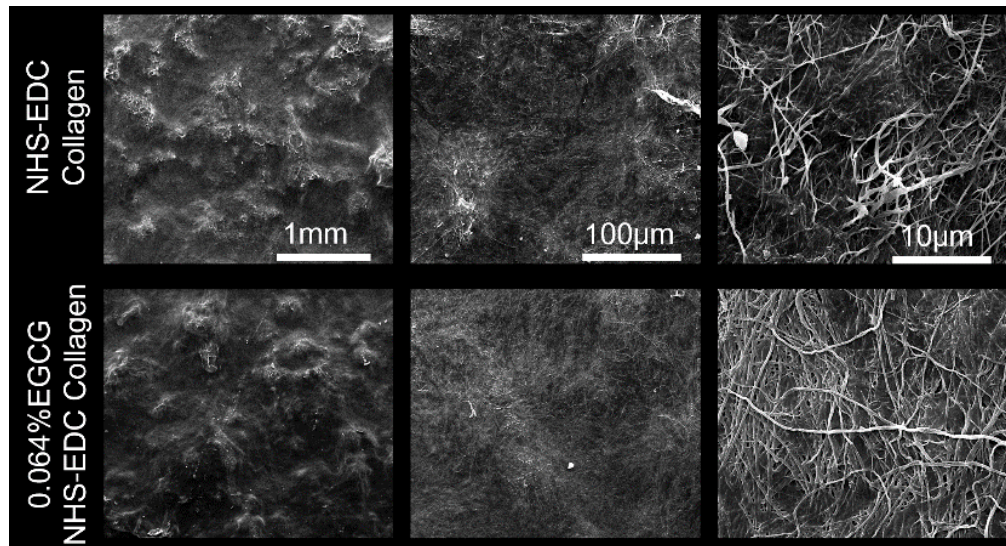
204 **2.9 Statistical Analysis**

205 Data are presented as mean + standard deviation. Statistical computation was
206 performed in GraphPad Prism 5.0 (GraphPad Software, San Diego, CA, USA) and
207 statistical significance was analyzed using analysis of variance followed by Tukey's
208 multiple comparison tests. Semi-quantitative data of immunofluorescence staining
209 and HE staining that did not follow a normal distribution were further analyzed with
210 Mann-Whitney U test. Unless otherwise noted, $p < 0.05$ was considered statistically
211 significant.

212 **3. Results**

213 **3.1 Surface morphology**

214 As shown in representative SEM images (**Fig. 2**), the surface morphology of
215 EDC/NHS collagen membranes exhibited a rough, disordered outlook, with fibers
216 randomly distributed. After treating with 0.064% EGCG, there were no notable
217 changes on the outlooks, while the arrangement of fibers appeared more ordered and
218 intact. In addition, we also found that smaller fiber branches extend from the
219 backbone when compared with those without EGCG treatment. These might be due to
220 the loading of EGCG hydrogen bonds formation between EGCG molecules and
221 collagen fibers.

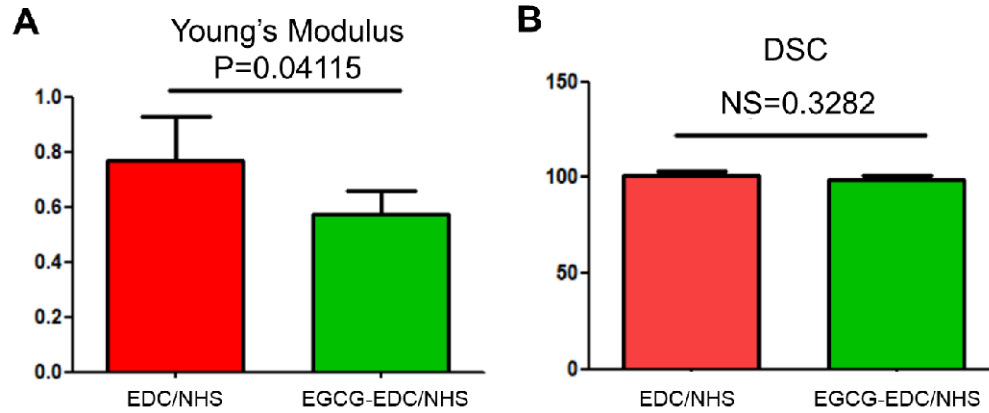


222
223 **Fig. 2.** SEM images of EDC/NHS collagen membrane and 0.064% EGCG loaded
224 EDC/NHS collagen membrane.

225 **3.2 Mechanical and chemical properties**

226 To examine the strength, stiffness and elasticity of the membranes, measurement of
227 US, UE and YM were carried out and the corresponding volumes were written in
228 **Table 2.** As US seemed relatively constant between the control and EGCG group,

229 both UE and YM showed different trends. The modification of 0.064% EGCG
230 strengthened the UE volume of collagen membranes, whereas weakened the YM
231 volume (**Fig. 3a**). Also, there were no statistical difference between membranes with
232 or without EGCG modification in result of DSC measurement (**Fig. 3b**). From results
233 of FTIR spectra and DSC measurement, it could be concluded that chemical
234 properties remain consistent before and after the treatment of 0.064% EGCG. The
235 FTIR spectra indicated that no structure changes had happened to collagen fibers
236 since the absorption peaked at 1235 cm^{-1} (tertiary structure) and 1450 cm^{-1}
237 (pyrrolidine ring vibrations) of EDC/NHS collagen membrane, and 0.064%
238 EGCG-EDC/NHS collagen membrane remained constant. Also, the ratio of 1235
239 $\text{cm}^{-1}/1450\text{ cm}^{-1}$ (**Table 3**) came out to be around 1.00, illustrating that the secondary
240 structure of collagen triple helix remained its integrity in both membranes, which
241 assured the great biological performance of collagen membranes (Figueiró, Góes,
242 Moreira, & Sombra, 2004).Therefore, it could be inferred that EGCG did not affect
243 the physicochemical property of collagen.



244

245 **Fig. 3.** Young's Modulus (a) and DSC statistics (b) of EDC/NHS collagen membrane
246 and 0.064% EGCG-EDC/NHS collagen membrane. NS= no significance.

247

3.3 Cell Viability

248

The results of CCK-8 staining showed the cell viability of raw 264.7 cells under pure

249

medium, 0.064% EGCG supplemented medium, EDC/NHS collagen membrane and

250

0.064% EGCG-EDC/NHS collagen membrane (**Fig. 4a**) from the first few minutes to

251

1 day. In the first hour, there was no significance between the groups. The

252

improvement of cell viability by EGCG was raised after culturing for 2 hr and the

253

following time points. In order to understand the effect of EGCG on cell viability

254

after culturing for longer time period, Calcein AM/Hoechst staining was conducted on

255

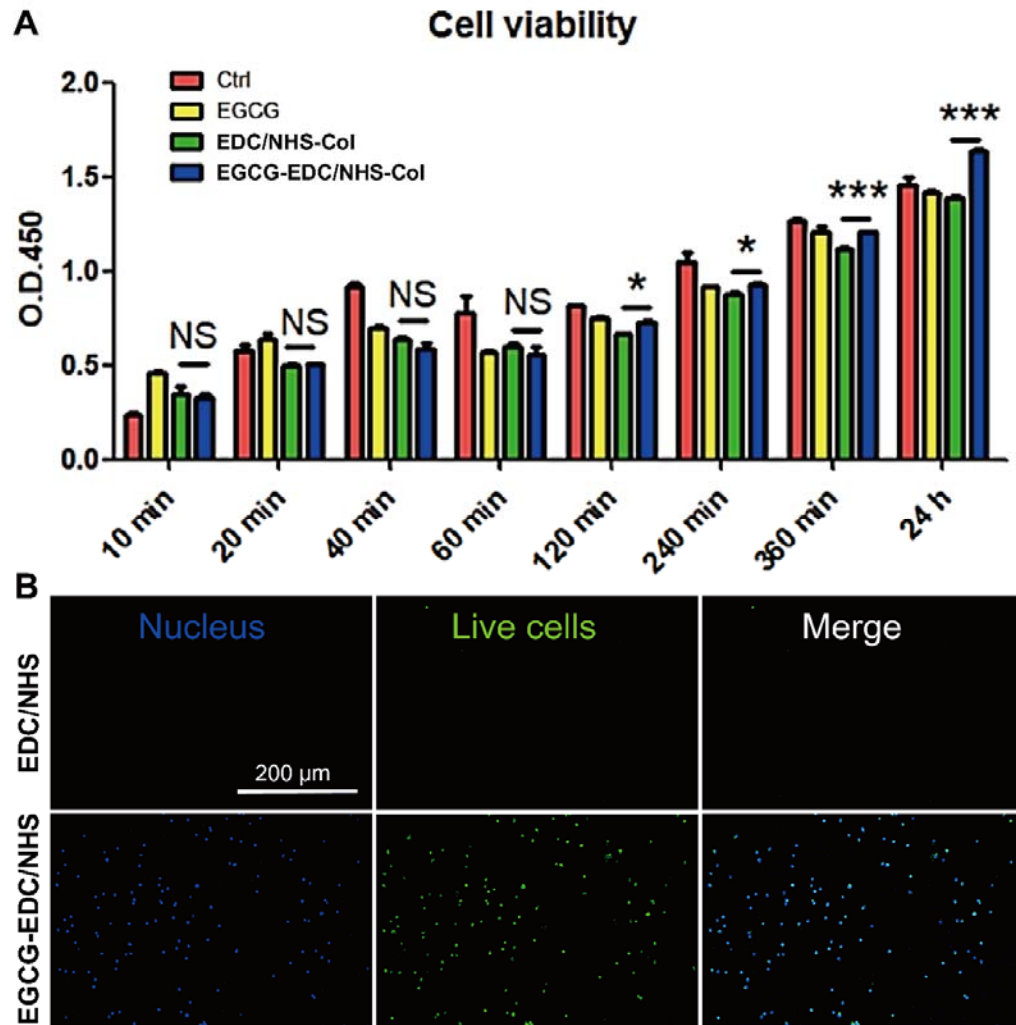
day 5 (**Fig. 4b**). The test results also showed the same trend with more live cells on

256

EGCG-EDC/NHS-Col comparing with EDC/NHS-Col, indicating that the addition of

257

EGCG was conducive to the performance of cell activities.



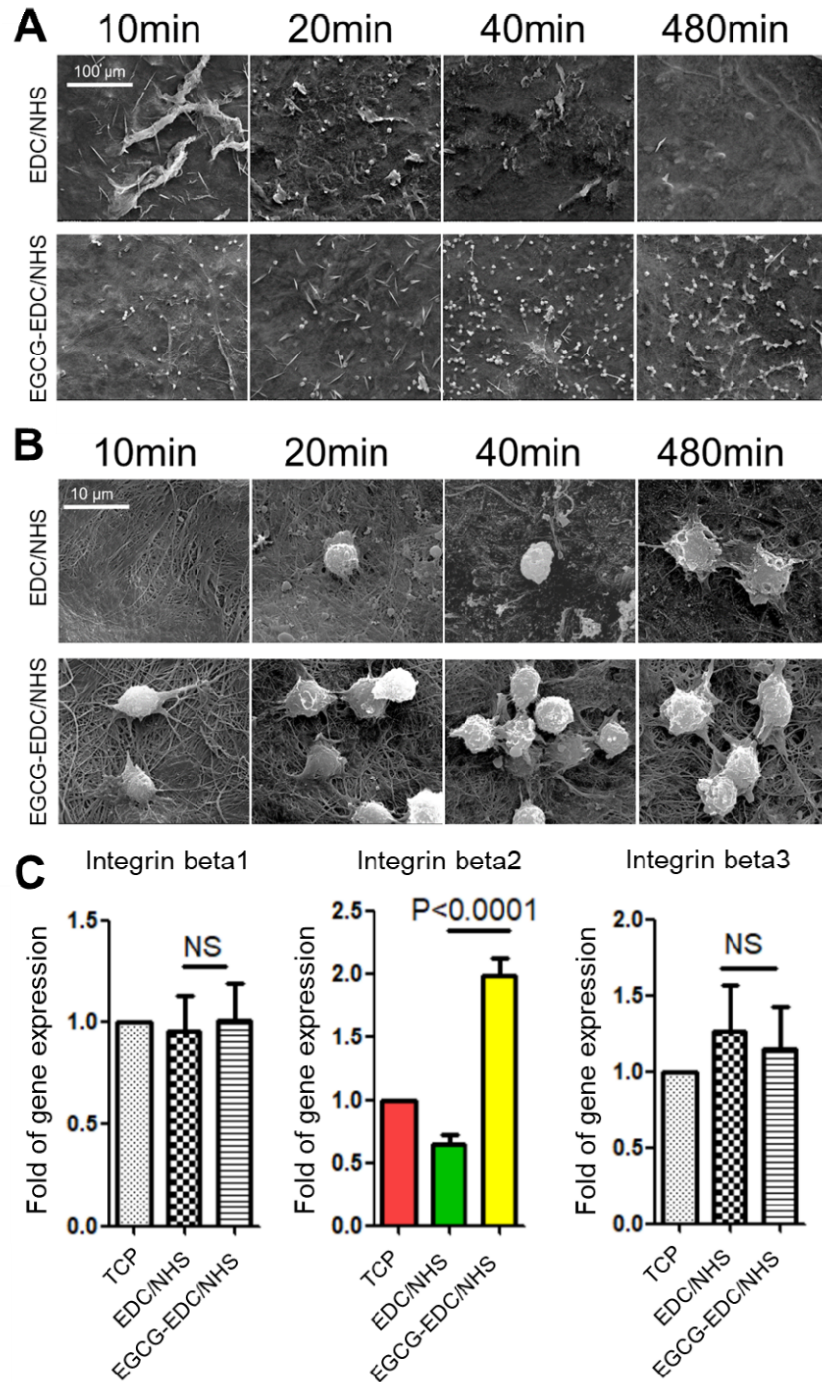
258

259 **Fig. 4.** CCK-8 results (a) and Calcein AM/Hoechst staining (b) of Raw 264.7 cultured
260 on different condition. Ctrl, standard medium; EGCG, 0.064% EGCG supplemented
261 medium; EDC/NHS-Col, EDC/NHS collagen membrane; EGCG-EDC/NHS-Col,
262 0.064% EGCG-EDC/NHS collagen membrane. Green, live cells; blue, nucleus. NS=
263 no significance, * $P < 0.05$, ** $P < 0.01$, *** $P < 0.001$, one-way ANOVA with Tukey's
264 multiple comparison test, $n = 3$ in each group.

265 3.4 Cell adhesion

266 To observe cell adhesion towards the membrane, SEM was used to generate the
267 morphology of Raw 264.7 cells cultured on membranes in 8 hr (**Fig. 5a&b**). It
268 elucidated that with the modification of EGCG, not only more cells adhered to the

269 surface but also a better spreading condition of cells was detected. Also, more
270 protrusions could be seen to seize the fibers even at very early incubation, compared
271 to that without EGCG. Considering integrins, the transmembrane molecules, with
272 large extracellular domains that are known to play a key role in adhesion between
273 cells and ECM (Changede & Sheetz, 2017; Tseng et al., 2018), expression levels of
274 integrin beta 1, 2 and 3 in Raw 264.7 cells were measured. The result showed that
275 there existed a boost of integrin beta 2 in the EGCG- EDC/NHS group, whereas no
276 differences appeared in the expression of integrin beta 1 and 3 with the treatment of
277 0.064% EGCG (**Fig. 5c**). These results suggested that 0.064% EGCG could enhance
278 the adhesion properties of EDC/NHS collagen membrane at early phases.



279

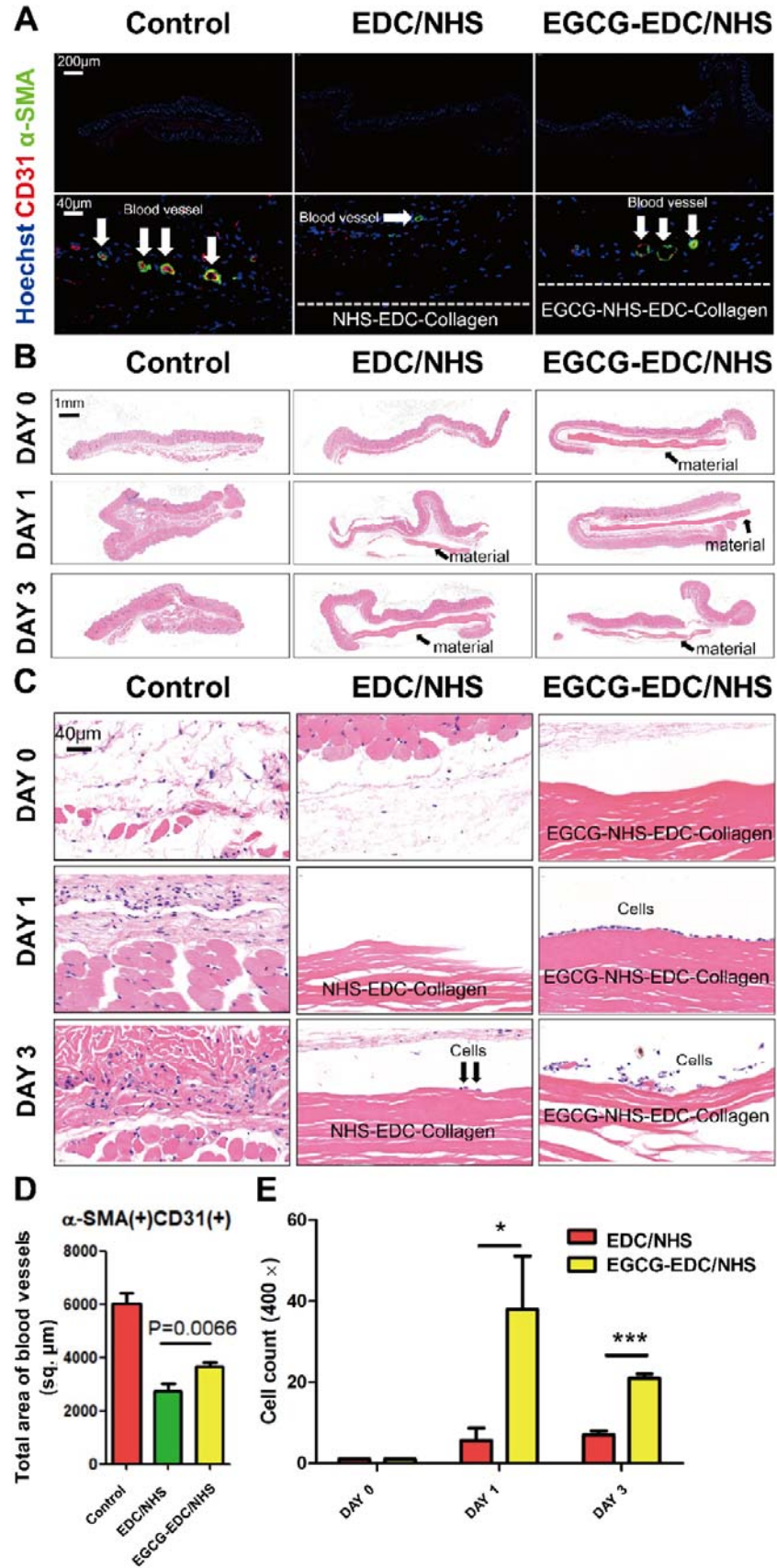
280 **Fig. 5.** SEM images of Raw 264.7 cells cultured on EDC/NHS and EGCG treated
281 EDC/NHS collagen membranes under low (a) and high (b) magnification, and the
282 expression levels of integrin beta 1, 2 and 3, after culturing on tissue culture plate
283 (TCP), EDC/NHS-Col and EGCG-EDC/NHS-Col for 10 mins (c), respectively. NS=
284 no significance.

285 **3.5 Promotion of revascularization**

286 We identified the ability of 0.064% EGCG EDC/NHS-Col to promote
287 revascularization by immunofluorescence staining of nuclei, vascular endothelial cell
288 marker CD31 and adventitial fibroblast marker α -SMA (Manetti et al., 2017). As
289 shown in **Fig. 6a**, more blood vessels were generated in EGCG-EDC/NHS-Col
290 compared to EDC/NHS-Col, meanwhile, as shown in **Fig. 6d**, the results of
291 semi-quantitative analysis of total blood vessel area showed that it was larger in 0.064%
292 EGCG EDC/NHS-Col than that in the EDC/NHS-Col ($p < 0.01$).

293 **3.6 Recruitment of monocyte/macrophage**

294 12 hours after the implantation, there were no visible cells recruited at surgical sites,
295 but with another 12 hours, we could see that around the membrane, a certain number
296 of immune cells were gathered, which was similar on 3-days post implantation (**Fig.**
297 **6c&d**). In addition, semi-quantitative cell counting revealed that in 1- and 3-days post
298 surgeries, 0.064% EGCG-EDC/NHS-Col recruited more monocytes/macrophages,
299 while EDC/NHS-Col was about one-third of the number of the experimental group
300 (**Fig. 6e**).



302 **Fig. 6.** Results of subcutaneous implantation. Immunofluorescence staining of α SMA
303 (green), CD31 (red) and Hoechst (blue) in subcutaneous implantation samples of
304 EDC/NHS-Col and EGCG-EDC/NHS-Col, control group refers to normal skin (a);
305 semi-quantitative analysis of total blood vessel area was calculated in each group (d).
306 Recruitment of monocyte/macrophage after subcutaneous implantation of EDC/NHS
307 collagen membrane and EGCG-EDC/NHS collagen membrane, control group
308 underwent a sham procedure. HE staining of subcutaneous tissue (b&c) and cell
309 counting of monocyte/macrophage (e) in NHS/EDC-Col and EGCG-EDC/NHS-Col
310 were conducted on day 0, 1, and 3 post implantations. Arrows indicate material (b)
311 and monocyte/macrophage (c). Statistical significance was analyzed using analysis of
312 variance followed by Tukey's multiple comparison tests and Mann-Whitney *U* test (*n*
313 = 5). Data are presented as mean + standard deviation. **P*<0.05, ****P*<0.001.

314 **4. Discussion**

315 To reconstruct alveolar bone deficiency, the application of biomaterials and certain
316 surgery are on account of its morphology and the severity of horizontal/ vertical bone
317 loss. When performing GBR, bone defect less than 6 mm is a prerequisite for
318 desirable outcome, whereas the complex case that is combined with vertical and
319 horizontal bone defect \leq 4mm, it is recommended to use crosslinked absorbable
320 membrane or non-absorbable membrane with bone filler to create appropriate repair
321 conditions (Tolstunov, Hamrick, Broumand, Shilo, & Rachmiel, 2019). In addition,
322 crosslinked membranes are more osteoinductive, with more bone marrow-multipotent
323 stromal cells attachment to the crosslinked membranes, better ALP activity, and
324 calcium deposition were observed compared with the non-crosslinked one (El-Jawhari,
325 Moisley, Jones, & Giannoudis, 2019). According to previous studies, the use of EDC
326 as crosslinker could not only prolong the integrity of the membrane, but also avoid

327 severe FBR, lack of vascularization in the early stage of healing and poor integration,
328 which are the fatal flaws of traditional cross-linking agents (Park et al., 2015). The
329 addition of NHS would improve EDC-mediated crosslinking, stabilize active
330 intermediates, and reduce side products for subsequent reactions (Grabarek & Gergely,
331 1990). However, the present EDC/NHS crosslinked collagen membrane lacks the
332 ability to regulate immune responses and induce osteoblast-related cell behavior.
333 Regarding cell behavior, EGCG has shown the ability to complement these two
334 aspects in our previous research as mentioned in the introduction. Thus, we attempted
335 to modify to EDC/NHS crosslinked collagen membrane with 0.064% EGCG. After
336 characterizing the material, results show that the backbone of collagen remains intact
337 and the strength of membranes is barely altered, whereas the stiffness is moderately
338 enhanced, though elasticity is slightly weakened. These not only ensure that the
339 membrane will not be too supple to tightly cover the substitutes, supporting bone
340 formation, but also verify that the chemical structure related to the biological activity
341 of collagen has not been destroyed, though the definite clinical effect needs
342 verification. Over the past decade, the ability of biomaterials to promote tissue
343 regeneration by regulating immune cells in advance has been confirmed, the
344 composition, physical and chemical properties, and surface morphology of which are
345 the critical factors that affect the foreign body reaction (FBR) after implantation. As

346 one of the dominant immune cells in the FBR, macrophages can acutely polarize into
347 different phenotypes according to the microenvironment created by the implant and
348 direct the accumulated cells' behaviors that strongly involve in tissue reconstruction
349 (Chu, Deng, Sun, Qu, & Man, 2017; Xie et al., 2020). The arrangement and diameter
350 of the fibers can significantly affect the behavior of macrophages. Anisotropic
351 membranes with thicker fibers have an increased tendency to oxidative degradation,
352 compared with the thinner and isotropic one (Wissing et al., 2019), more macrophages
353 adherence on the align compared with the random and the smaller fibers also have
354 been proved with better biocompatibility as thinner fibrous capsule and abundant
355 volume of blood vessel formation (Saino et al., 2011). In this article, we found that the
356 surface morphology of EGCG-EDC/NHS-Col has been altered with smaller fiber
357 branches extended from the backbone and the arrangement became more coherent,
358 which may account for the cell viability and adherence. Under the electron
359 microscope, the viability of RAW 264.7 on EGCG-EDC/NHS-Col is significantly
360 higher than any other groups at all detection points during 2-24 hours after
361 implantation. Not only did more macrophages adhere to membrane with the treatment
362 of EGCG, but the adhered macrophages were activated at an early stage (20min) with
363 many protrusions, and which is also confirmed by PCR detection. Also, more
364 monocyte/macrophage recruitment could be seen on EGCG-EDC/NHS-Col in the *in*

365 *vivo* subcutaneous implantation. As researchers have found that the onset of
366 neovascularization greatly depends on macrophage and its coherent phenotypic switch
367 (Spiller et al., 2014; Spiller, Freytes, & Vunjak-Novakovic, 2015), we hypothesize the
368 promising angiogenesis is result from the recruitment of macrophages which cannot
369 be excluded considering the microstructure of EGCG-EDC/NHS-Col. Of note, in our
370 previous study, the modification of EGCG was highly competent at promoting
371 vascularization that involved the secretion of M2-related chemokines (Chu et al.,
372 2018). The formation of blood vessel could offer nutrient, stem cells and oxygen
373 supply and waste discharge, vastly improving the regenerative response. Therefore,
374 our efforts are directed at macrophages and the outcome of vascularization as primary
375 study towards the developed EGCG modified EDC/NHS collagen membrane. And
376 our results showed that the modification of EGCG is beneficial for cell viability,
377 adhesion and vessel formation in both *in vitro* RAW 264.7 culture experiment and in
378 *vivo* subcutaneous implantation. The great biocompatibility of EGCG modified
379 EDC/NHS collagen guided bone regeneration membrane is stated without
380 compromising the advantages of collagen itself. Furthermore, our results
381 demonstrated the modified membranes could significantly affect the attachment of
382 macrophages and enhance its viability both *in vivo* and *in vitro*, which might be
383 related to the formation of vessels. However, the phenotypes of macrophages and

384 mechanisms of angiogenesis need further investigation. In short, we develop a
385 biomaterial that can promote the early recruitment of macrophages and the formation
386 of blood vessels, possessing great potential for bone regeneration in the field of
387 implant dentistry.

388 **5. Conclusion**

389 In conclusion, with the modification of EGCG, EDC/NHS collagen guided bone
390 regeneration membrane can better promote cell adhesion and improve cell viability,
391 which is confirmed in our experiments that living cells attach to it and the expression
392 of adhesion-related integrin is indeed increased. In addition, there was a statistically
393 significant difference in angiogenesis after membrane implantation. The benefits
394 mentioned above do not exclude the presence of smaller collagen fibers, but this
395 different microstructure does not damage the chemical structure of the collagen itself,
396 though the specific effect needs further exploration.

397 **Funding information**

398 This work was supported by Research and Develop Program, West China Hospital of
399 Stomatology Sichuan University (No.LCYJ2019-19); the Fundamental Research
400 Funds for the Central Universities (No. 2082604401239)

401 **Statement of conflict of interest**

402 There are no conflicts of interest related to this manuscript.

404 **Table 1. Nucleotide primers used for quantitative polymerase chain reaction.**

Genes	Oligonucleotide sequence
Integrin b1	Forward: CCAAGTGGGACACGGGTGA
	Reverse: CTGCTGCTGTGAGCTTGGTG
Integrin b2	Forward: GCAGCAGAAGGACGGAAACG
	Reverse: AGGGGGTTGTCGTTGTTCCA
Integrin b3	Forward: AGACAGCGCCCAGATCACTC
	Reverse: GCCAATCCGAAGGTTGCTGG

405

406

407 **Table 2. Mechanical properties of membranes.**

Groups	Ultimate Stress (MPa)	Ultimate elongation (%)	Young's modulus
EDC/NHS-Col	18.32±3.12	22.44±3.12	0.77±0.16
EGCG-EDC/NHS-Col	18.18±2.97	29.29±2.78	0.57±0.09

408

409

410 **Table 3. FTIR ratio at the bands of 1235 cm⁻¹ and 1450 cm⁻¹**

Groups	1235/1450
NHS/EDC-Col	1.001±0.002
EGCG-NHS/EDC-Col	0.989±0.003

411

412 **Reference**

- 413 Akhshabi, S., Biazar, E., Singh, V., Keshel, S. H., & Geetha, N. (2018). The effect of the carbodiimide
414 cross-linker on the structural and biocompatibility properties of collagen-chondroitin sulfate
415 electrospun mat. *International journal of nanomedicine*, *13*, 4405-4416.
- 416 Bax, D. V., Davidenko, N., Gullberg, D., Hamaia, S. W., Farndale, R. W., Best, S. M., & Cameron, R. E.
417 (2017). Fundamental insight into the effect of carbodiimide crosslinking on cellular
418 recognition of collagen-based scaffolds. *Acta biomaterialia*, *49*, 218-234.
- 419 Changede, R., & Sheetz, M. (2017). Integrin and cadherin clusters: A robust way to organize adhesions
420 for cell mechanics. *BioEssays : news and reviews in molecular, cellular and developmental*
421 *biology*, *39*(1), 1-12.
- 422 Chu, C., Deng, J., Sun, X., Qu, Y., & Man, Y. (2017). Collagen Membrane and Immune Response in
423 Guided Bone Regeneration: Recent Progress and Perspectives. *Tissue engineering. Part B,*
424 *Reviews*, *23*(5), 421-435.
- 425 Chu, C., Deng, J., Xiang, L., Wu, Y., Wei, X., Qu, Y., & Man, Y. (2016). Evaluation of
426 epigallocatechin-3-gallate (EGCG) cross-linked collagen membranes and concerns on
427 osteoblasts. *Materials science & engineering. C, Materials for biological applications*, *67*,
428 386-394.
- 429 Chu, C., Liu, L., Rung, S., Wang, Y., Ma, Y., Hu, C., . . . Qu, Y. (2020). Modulation of foreign body
430 reaction and macrophage phenotypes concerning microenvironment. *Journal of biomedical*
431 *materials research. Part A*, *108*(1), 127-135.
- 432 Chu, C., Liu, L., Wang, Y., Wei, S., Wang, Y., Man, Y., & Qu, Y. (2018). Macrophage phenotype in the
433 epigallocatechin-3-gallate (EGCG)-modified collagen determines foreign body reaction.
434 *Journal of Tissue Engineering and Regenerative Medicine*, *12*(6), 1499-1507.
- 435 Chu, C., Wang, Y., Wang, Y., Yang, R., Liu, L., Rung, S., . . . Qu, Y. (2019). Evaluation of
436 epigallocatechin-3-gallate (EGCG) modified collagen in guided bone regeneration (GBR)
437 surgery and modulation of macrophage phenotype. *Materials science & engineering. C,*
438 *Materials for biological applications*, *99*, 73-82.
- 439 El-Jawhari, J. J., Jones, E., & Giannoudis, P. V. (2016). The roles of immune cells in bone healing;
440 what we know, do not know and future perspectives. *Injury-international Journal of the Care*
441 *of the Injured*, *47*(11), 2399-2406.
- 442 El-Jawhari, J. J., Moisley, K., Jones, E., & Giannoudis, P. V. (2019). A crosslinked collagen membrane
443 versus a non-crosslinked bilayer collagen membrane for supporting osteogenic functions of
444 human bone marrow-multipotent stromal cells. *European cells & materials*, *37*, 292-309.
- 445 Eskan, M. A., Girouard, M. E., Morton, D., & Greenwell, H. (2017). The effect of membrane exposure
446 on lateral ridge augmentation: a case-controlled study. *International journal of implant*
447 *dentistry*, *3*(1), 26.
- 448 Figueiró, S. D., Góes, J. C., Moreira, R. A., & Sombra, A. S. B. (2004). On the physico-chemical and
449 dielectric properties of glutaraldehyde crosslinked galactomannan–collagen films.

- 450 *Carbohydrate Polymers*, 56(3), 313-320.
- 451 Grabarek, Z., & Gergely, J. (1990). Zero-length crosslinking procedure with the use of active esters.
- 452 *Analytical biochemistry*, 185(1), 131-135.
- 453 Honda, Y., Takeda, Y., Li, P., Huang, A., Sasayama, S., Hara, E., . . . Tanaka, T. (2018).
- 454 Epigallocatechin Gallate-Modified Gelatin Sponges Treated by Vacuum Heating as a Novel
- 455 Scaffold for Bone Tissue Engineering. *Molecules*, 23(4), 876.
- 456 Kurashima, Y., & Kiyono, H. (2017). Mucosal Ecological Network of Epithelium and Immune Cells
- 457 for Gut Homeostasis and Tissue Healing. *Annual review of immunology*, 35, 119-147.
- 458 Lagha, A. B., & Grenier, D. (2019). Tea polyphenols protect gingival keratinocytes against
- 459 TNF- α -induced tight junction barrier dysfunction and attenuate the inflammatory response of
- 460 monocytes/macrophages. *Cytokine*, 115, 64-75.
- 461 Liao, S., Tang, Y., Chu, C., Lu, W., Baligen, B., Man, Y., & Qu, Y. (2020). Application of green tea
- 462 extracts epigallocatechin-3-gallate in dental materials: Recent progress and perspectives.
- 463 *Journal of biomedical materials research. Part A*.
- 464 Lin, S. Y., Kang, L., Wang, C. Z., Huang, H. H., Cheng, T. L., Huang, H. T., . . . Chen, C. H. (2018).
- 465 (-)-Epigallocatechin-3-Gallate (EGCG) Enhances Osteogenic Differentiation of Human Bone
- 466 Marrow Mesenchymal Stem Cells. *Molecules*, 23(12), 3221.
- 467 Manetti, M., Romano, E., Rosa, I., Guiducci, S., Bellando-Randone, S., De Paulis, A., . . .
- 468 Matucci-Cerinic, M. (2017). Endothelial-to-mesenchymal transition contributes to endothelial
- 469 dysfunction and dermal fibrosis in systemic sclerosis. *Annals of the rheumatic diseases*, 76(5),
- 470 924-934.
- 471 Melcher, A. H. (1976). On the repair potential of periodontal tissues. *Journal of periodontology*, 47(5),
- 472 256-260.
- 473 Meyer, M. (2019). Processing of collagen based biomaterials and the resulting materials properties.
- 474 *Biomedical engineering online*, 18(1), 24.
- 475 Park, J. Y., Jung, I. H., Kim, Y. K., Lim, H. C., Lee, J. S., Jung, U. W., & Choi, S. H. (2015). Guided
- 476 bone regeneration using 1-ethyl-3-(3-dimethylaminopropyl) carbodiimide (EDC)-cross-linked
- 477 type-I collagen membrane with biphasic calcium phosphate at rabbit calvarial defects.
- 478 *Biomaterials research*, 19, 15.
- 479 Saino, E., Focarete, M. L., Gualandi, C., Emanuele, E., Cornaglia, A. I., Imbriani, M., & Visai, L.
- 480 (2011). Effect of electrospun fiber diameter and alignment on macrophage activation and
- 481 secretion of proinflammatory cytokines and chemokines. *Biomacromolecules*, 12(5),
- 482 1900-1911.
- 483 Spiller, K. L., Anfang, R. R., Spiller, K. J., Ng, J., Nakazawa, K. R., Daulton, J. W., &
- 484 Vunjak-Novakovic, G. (2014). The role of macrophage phenotype in vascularization of tissue
- 485 engineering scaffolds. *Biomaterials*, 35(15), 4477-4488.
- 486 Spiller, K. L., Freytes, D. O., & Vunjak-Novakovic, G. (2015). Macrophages modulate engineered
- 487 human tissues for enhanced vascularization and healing. *Annals of biomedical engineering*,

- 488 43(3), 616-627.
- 489 Tolstunov, L., Hamrick, J. F. E., Broumand, V., Shilo, D., & Rachmiel, A. (2019). Bone Augmentation
490 Techniques for Horizontal and Vertical Alveolar Ridge Deficiency in Oral Implantology. *Oral*
491 *and maxillofacial surgery clinics of North America*, 31(2), 163-191.
- 492 Tseng, H. Y., Samarelli, A. V., Kammerer, P., Scholze, S., Ziegler, T., Immler, R., . . . Böttcher, R. T.
493 (2018). LCP1 preferentially binds clasped α M β 2 integrin and attenuates leukocyte adhesion
494 under flow. *Journal of cell science*, 131(22), jcs218214.
- 495 Wang, L., Yang, G., Yuan, L., Yang, Y., & Zhao, H. (2018). Green Tea Catechins Effectively Altered
496 Hepatic Fibrogenesis in Rats by Inhibiting ERK and Smad1/2 Phosphorylation. *Journal of*
497 *agricultural and food chemistry*, 67(19), 5437-5445
- 498 Wessing, B., Lettner, S., & Zechner, W. (2018). Guided Bone Regeneration with Collagen Membranes
499 and Particulate Graft Materials: A Systematic Review and Meta-Analysis. *The International*
500 *journal of oral & maxillofacial implants*, 33(1), 87–100.
- 501 Wissing, T. B., Bonito, V., van Haaften, E. E., van Doeselaar, M., Brugmans, M., Janssen, H. M., . . .
502 Smits, A. (2019). Macrophage-Driven Biomaterial Degradation Depends on Scaffold
503 Microarchitecture. *Frontiers in bioengineering and biotechnology*, 7, 87.
- 504 Wu, Y. R., Choi, H. J., Kang, Y. G., Kim, J. K., & Shin, J. W. (2017). In vitro study on
505 anti-inflammatory effects of epigallocatechin-3-gallate-loaded nano- and microscale particles.
506 *International journal of nanomedicine*, 12, 7007-7013.
- 507 Xie, Y., Hu, C., Feng, Y., Li, D., Ai, T., Huang, Y., . . . Tan, J. (2020). Osteoimmunomodulatory effects
508 of biomaterial modification strategies on macrophage polarization and bone regeneration.
509 *Regenerative biomaterials*, 7(3), 233-245.